Paleoceanography and Paleoclimatology

RESEARCH ARTICLE
10.1029/2019PA003770

20th Century $\delta^{18}O$ Seawater and Salinity Variations Reconstructed From Paired $\delta^{18}O$ and Sr/Ca Measurements of a La Reunion Coral

M. Pfeiffer[1], L. Reuning[1], J. Zinke[2,3,4,5], D. Garbe-Schönberg[1], M. Leupold[6], and Wolf-Christian Dullo[7]

[1]Institute of Geosciences, Kiel University, Kiel, Germany, [2]School of Geography, Geology and the Environment, University of Leicester, Leicester, UK, [3]Molecular and Life Sciences, Curtin University, Perth, Western Australia, Australia, [4]Australian Institute of Marine Science, Townsville, Queensland, Australia, [5]School of Geography, Archaeology and Environmental Studies, University of Witwatersrand, Johannesburg, South Africa, [6]Geological Institute, RWTH Aachen, Aachen, Germany, [7]GEOMAR, Kiel, Germany

Abstract Sea surface salinity (SSS) is an important variable in the global ocean circulation. However, decadal to interdecadal changes in SSS are not well understood due to the lack of instrumental data. Here we reconstruct SSS from a paired, bimonthly resolved coral $\delta^{18}O$ and Sr/Ca record from La Reunion Island that extends from 1913 to 1995. Coral Sr/Ca correlates with regional sea surface temperature (SST) back to 1966, when instrumental coverage is good, while coral $\delta^{18}O$ does not. The slope of the monthly (annual mean) coral Sr/Ca-SST regression is −0.040 mmol/mol per 1 °C (−0.068 mmol/mol per 1 °C) consistent with published estimates of the Sr/Ca-SST relationship. Coral Sr/Ca suggest a warming of 0.39 °C since 1913. $\delta^{18}O$ seawater is calculated by subtracting the temperature component from measured coral $\delta^{18}O$, using coral Sr/Ca as well as historical SST products. The derived $\delta^{18}O$ seawater reconstructions are correlated ($r > 0.6$), and all show a significant shift in the midtwentieth century (−0.17‰ to −0.19‰), indicating a freshening of SSS by 0.7 psu. However, the timing of this shift depends on the temperature component and varies from 1947 ($\delta^{18}O$ seawater calculated with historical SST) to the late 1950s ($\delta^{18}O$ seawater calculated with coral Sr/Ca). Coral Sr/Ca shows warm temperature anomalies in the mid-1950s, while historical SST products show warm anomalies from 1940 to 1945 followed by cooling in the 1950s, a pattern typical for the World War II bias. This suggests that historical SST may bias reconstructions of $\delta^{18}O$ seawater and SSS from corals.

Key Points:
- La Reunion coral oxygen isotopes record changes in the isotopic composition of seawater/salinity, while Sr/Ca ratios record temperature
- The coral record suggests a significant freshening in the mid-20th century
- Potential biases in historical temperature data may influence $\delta^{18}O$ seawater/salinity reconstructions from corals

Supporting Information:
- Supporting Information S1
- Data Set S1

Correspondence to:
M. Pfeiffer,
miriam.pfeiffer@ifg.uni-kiel.de

Citation:
Pfeiffer, M., Reuning, L., Zinke, J., Garbe-Schönberg, D., Leupold, M., & Dullo, W.-C. (2019). 20th century $\delta^{18}O$ seawater and salinity variations reconstructed from paired $\delta^{18}O$ and Sr/Ca measurements of a La Reunion coral. *Paleoceanography and Paleoclimatology*, *34*, 2183–2200. https://doi.org/10.1029/2019PA003770

Received 17 SEP 2019
Accepted 20 NOV 2019
Accepted article online 22 NOV 2019
Published online 26 DEC 2019

1. Introduction

Sea surface salinity (SSS) plays an important role in ocean circulation, advection, thermodynamics, and mixed layer depth and can be used as a proxy for the hydrological cycle (Bingham et al., 2012; Han & McCreary, 2001; Nyadjro & Subrahmanyam, 2016). However, measurements of salinity are sparse and often inadequate compared to those of sea surface temperature (SST), although both are important for understanding oceanic processes and air-sea interactions (Nyadjro & Subrahmanyam, 2016). Satellite-based measurements of SSS such as the Aquarius data (Melnichenko et al., 2014, 2015) currently cover less than a decade, making it difficult to assess year-to-year or longer-term variations and the processes that drive them.

The Indonesian Throughflow (ITF) brings fresher, warmer waters from the Pacific into the Indian Ocean south of 5°S, which are carried westward by the South Equatorial Current (SEC) and influence salinity in the western Indian Ocean between 5°S and 20°S (Sprintall et al., 2009). In addition, abundant precipitation associated with the seasonal movement of the Intertropical Convergence Zone (ITCZ) influences SSS (Srivastava et al., 2007). As a result, Indian Ocean surface salinity shows very large variability across a range of spatial and temporal scales (Han & McCreary, 2001; Nyadjro & Subrahmanyam, 2016; Schott et al., 2009). To reveal the temporal dynamics of SSS in the Indian Ocean on time scales longer than interannual, it is necessary to reconstruct surface salinity from geochemical proxy records that extend beyond the past decade.

Coral skeletons contain a suite of isotopic and trace elemental indicators that provide high resolution (seasonal to monthly) proxy records spanning several decades to centuries and are an ideal archive to reconstruct past changes in SSS (e.g., Cahyarini et al., 2008; Cahyarini et al., 2014; Felis et al., 2018; Hennekam et al., 2018; Nurhati et al., 2011). The coral oxygen isotopic composition ($\delta^{18}O$) is sensitive to SST and the $\delta^{18}O$

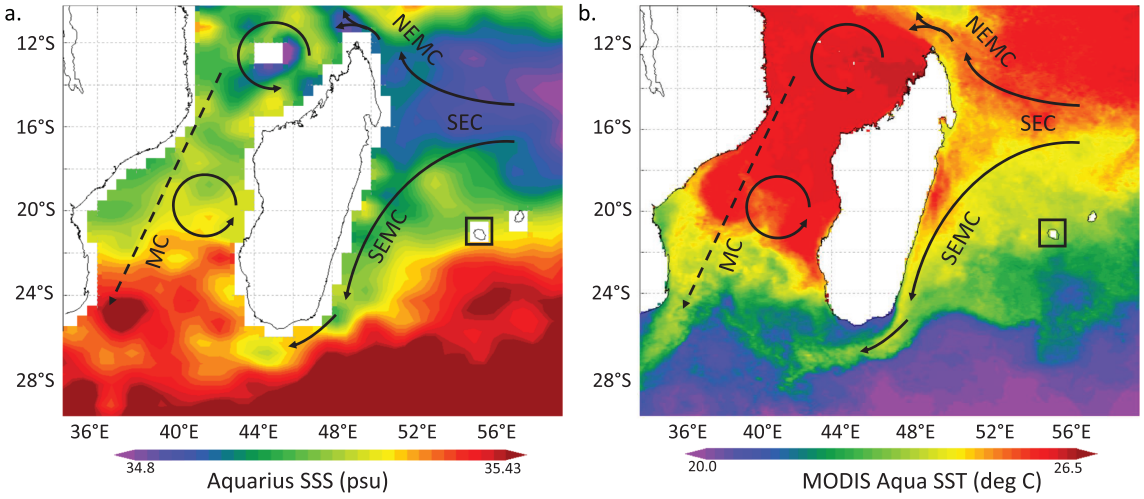

Figure 1. Monthly SSS and SST in the SW Indian Ocean. (a) Map of mean monthly SSS (Aquarius OISSS, 1° × 1° grid) and (b) mean monthly SST (MODIS Aqua daytime SST, 4 km resolution) during August 2013 in the SW Indian Ocean. The SEC can be seen as a low-salinity, warm water current that bifurcates at the coast of Madagascar. The location of La Reunion is indicated by a black rectangle. Charts computed with Live Access Server LAS8.6 (http://apdrc.soest.hawaii.edu, date of access 26 March 2019).

of seawater ($\delta^{18}O_{sw}$), while coral Sr/Ca ratios primarily reflect changes in SST (e.g., Corrège, 2006). When combined, paired coral $\delta^{18}O$ and Sr/Ca measurements allow the reconstruction of $\delta^{18}O_{sw}$ by removing the SST contribution from measured coral $\delta^{18}O$ (e.g., Cahyarini et al., 2008; Nurhati et al., 2011). In the tropical oceans, $\delta^{18}O_{sw}$ is linearly related to SSS (Schmidt, 1998; Srivastava et al., 2007), as both increase with evaporation and decrease through admixture of low-$\delta^{18}O$ freshwater. $\delta^{18}O_{sw}$ estimated from coral skeletons is therefore used to infer decadal to centennial changes of SSS (Cahyarini et al., 2014; Felis et al., 2018; Hennekam et al., 2018; Nurhati et al., 2011). Given the lack of historical SSS data, the reconstruction of $\delta^{18}O_{sw}$ is an important contribution of coral skeletal archives for our understanding of ocean circulation and climate variability. However, at present only a handful of coral $\delta^{18}O_{sw}$ and SSS reconstructions are available from the tropical Indian Ocean (Cahyarini et al., 2014; Hennekam et al., 2018; Watanabe et al., 2017; Zinke et al., 2008). While interannual changes of coral $\delta^{18}O_{sw}$ have been linked to changes in the surface freshwater balance driven by interannual modes of climate variability such as ENSO and the Indian Ocean Dipole (e.g., Abram et al., 2008; Cahyarini et al., 2014; Watanabe et al., 2019), the drivers of lower-frequency changes of $\delta^{18}O_{sw}$ are not always known.

Here we present the first paired coral $\delta^{18}O$ and Sr/Ca record from La Reunion Island (SW Indian Ocean, 55° E, 21°S) that covers the time period from 1995 to 1913. La Reunion lies at the southern margin of the SEC that carries warm, fresh water from the Eastern Indian Ocean/Maritime continent and the ITF toward the western margin of the Indian Ocean basin (Figure 1). To the south of La Reunion surface waters are saltier and cooler (Figure 1). The stable oxygen isotopic composition of the Reunion coral was analyzed and published in a previous study (Pfeiffer et al., 2004). This coral $\delta^{18}O$ record showed multidecadal variations that were opposite to the temperature signal expected from local SST data and were interpreted as low-frequency variations of δ^{18}Osw and SSS. Time-dependent variations of δ^{18}Osw suggested a possible link to the Pacific Decadal Oscillation (PDO), which may influence the southern tropical and subtropical Indian Ocean via ITF transport and/or changes in the surface wind field (Han et al., 2014; Sprintall et al., 2009). The coral Sr/Ca data presented in this study provide new constraints on the timing and magnitude of $\delta^{18}O_{sw}$ and SSS changes at La Reunion, and their potential linkage to large-scale climatic modes.

2. Study Area

Reunion is located about 800 km east of Madagascar (Figure 1). It is the youngest and most southwesterly volcanic island of the Mascarene group and its highest peak is 3,069 m. The high relief causes pronounced windward/leeward effects (Figure S1 in the supporting information; Pfeiffer et al., 2004). La

Reunion is located close to the southernmost limit of coral reef growth and compared to the other Mascarene Islands reef development is poor. 10–12 km of fringing reef are found on the west coast (Figure S2), that is, on the leeward side, where mean SSTs are slightly higher than on the southeast coast, which faces the southeasterly (SE) trade winds (Figure S1). Moderate Resolution Imaging Spectroradiometer (MODIS) Aqua daytime SST (4 km; Werdell et al., 2013) shows a mean temperature difference of 0.48 °C between the SE and NW coast of La Reunion (not shown).

The SE trade winds are blowing year-round from a generally east-southeastern direction (Pfeiffer et al., 2004; Schott et al., 2009). The SE trades are strongest in austral winter, lasting from May to October, when the ITCZ is situated over the Indian subcontinent. In austral summer, the ITCZ forms south of the equator and occasionally influences La Reunion (Schott et al., 2009).

Reunion lies at the southern margin of the SEC, which flows westward between 10°S and 20°S and forms the northern branch of the subtropical Indian Ocean gyre (Figure 1, Figure S3; Schott et al., 2009). The SEC is the most powerful and persistent current in the Indian Ocean. It is strengthened by the ITF and carries warm, fresh water toward the western Indian Ocean (Sprintall et al., 2009). The SEC bifurcates near the midpoint of the east Madagascan coast, and the southward flowing branch, known as the Southeast Madagascar current (SEMC), feeds the Agulhas current (Schott et al., 2009). The northern branch rounds the northern tip of Madagascar and turns southward to become the Mozambique current, although part of it continues north (Schott et al., 2009). Salinity gradients around La Reunion result from the mixing of fresh (and warm) water from the SEC/SEMC to the North and West of the Island with the saltier, subtropical (and colder) waters in the South (Figures 1 and S3). The mixing of these water masses causes eddies (Figure 1; Pfeiffer et al., 2004). Combined salinity and $\delta^{18}O_{sw}$ measurements from the western Indian Ocean show that $\delta^{18}O_{sw}$ follows the SSS pattern, with low $\delta^{18}O_{sw}$ and SSS in the region of the SEC between 10° and 20°S and high $\delta^{18}O_{sw}$ and SSS south of 20°S (Srivastava et al., 2007).

2.1. Satellite Data of SST and SSS

The mean annual temperature range at La Reunion is 4.6 °C (OI SST, 1° × 1° grid, 1982–2018; Reynolds et al., 2002), with minimum temperatures of 23.34 °C in austral winter (August) and maximum temperatures of 27.96 °C in austral summer (February, Figure 2). Interannual variations of sea surface temperature are an order of magnitude smaller than seasonal variations (Figure 2). The 1σ standard deviation of monthly OI SST anomalies is 0.46 °C.

Time series of instrumental SSS are now available from satellites and reanalysis data. Figure 2 compares gridded SSS from the Aquarius satellite, available from 2011 to 2015 (Melnichenko et al., 2014, 2015), and Met Office Hadley Centre EN SSS (Good et al., 2013) with climatological data from the World Ocean Atlas 2013 for the period from 2000 to 2018. In the grid including La Reunion, climatological SSS from the World Ocean Atlas 2013 shows a mean seasonal cycle of 0.14 psu, with maximum values following austral winter (35.12 psu, August–December), and minimum values in austral summer (34.98, April). However, Aquarius satellite data and EN SSS show that in many years, seasonal variations are poorly defined. Interannual variations exceed the seasonal variations by a factor of 2 or more (Figure 2). EN SSS has a maximum of 35.55 in February 2012, and a minimum of 34.80 in April 2010, amounting to a difference >0.7 psu.

2.2. Historical Temperature Data in the SW Indian Ocean

Instrumental SST data in the SW Indian Ocean are sparse. Figure 3 shows International Comprehensive Ocean-Atmosphere Data Set (ICOADS) SST (version 2.5) averaged over the region 55–80°E, 5–20°S (Woodruff et al., 2011). The number of observations drops abruptly in 1966. Prior to 1950, the ICOADS SST record is discontinuous. There are only a few months with data during/after World War II. The ICOADS data form the basis for all available reconstructions of historical SSTs that cover the twentieth century (Thompson et al., 2008). However, ICOADS data are biased due to changes in the measurement procedures of SST over time, most notably the shift from bucket to engine room intake measurements in the midtwentieth century (Thompson et al., 2008). These biases continue to pose a problem for twentieth century SST reconstructions from historical data, most notably during and after World War II (e.g., Pfeiffer et al., 2017; Thompson et al., 2008).

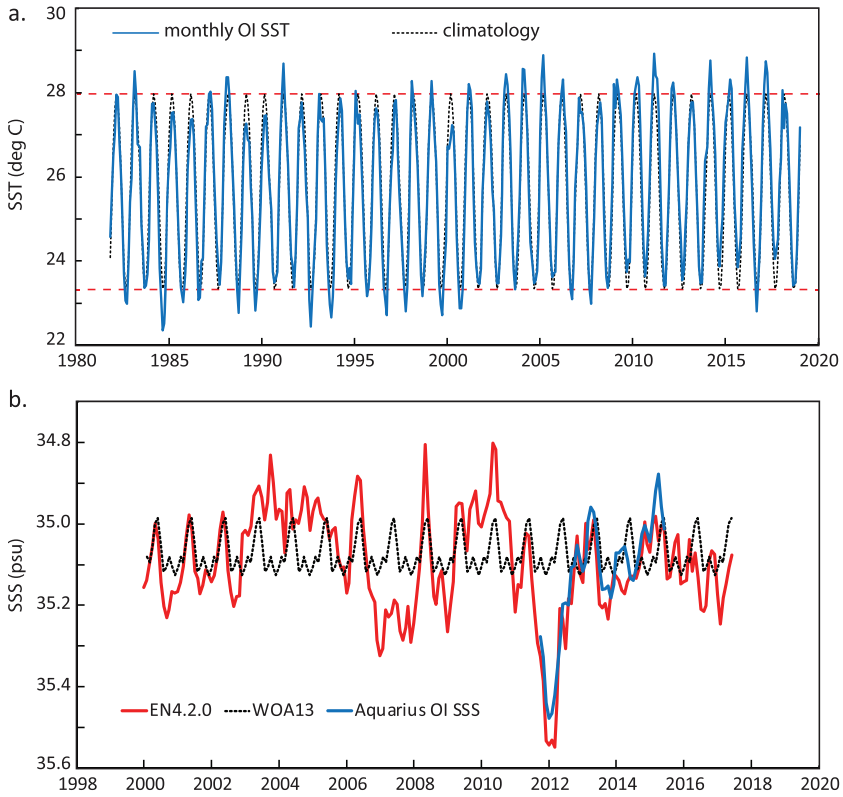

Figure 2. Satellite data of SST and SSS at La Reunion. (a) Monthly SST from the OI SST data set for the time period from 1982 to 2018 (blue line) (1° × 1° grid centered at 55°E, 21°S; Reynolds et al., 2002) compared with climatological SST (black dashed line). Note the large seasonal cycle (>4.5 °C) and the comparatively small interannual variations. (b) Monthly SSS from EN 4.2.0 (red line; Good et al., 2013) and Aquarius OI SSS (blue line; Melnichenko et al., 2014, 2015) compared with climatological SSS from the World Ocean Atlas 2013 (black dashed line). Interannual variations of SSS may be more than twice as large as seasonal variations. See text for discussion.

Figure 3c shows Hadley Centre Global Sea Ice and Sea Surface Temperature version 3 (HadSST3) data for the SW Indian Ocean (55–80°E, 5–20°S; Kennedy et al., 2011a, 2011b). HadSST3 is produced by taking in situ measurements of SST from ships and buoys from the ICOADS database. The measurements are converted to anomalies by subtracting climatological values from the data, and by calculating a robust average of the resulting anomalies on a 5° × 5° degree monthly grid. After gridding the anomalies, bias adjustments are applied to reduce the effects of spurious trends caused by changes in SST measuring practices. These bias adjustments include a correction of the World War II bias. There is no interpolation to fill in missing grid cells, and this results in coverage gaps. In the SW Indian Ocean, coverage gaps become a problem in the World War II period (Figure 3).

The Extended Reconstructed Sea Surface Temperature (ERSST) version 5 is a global, monthly sea surface temperature product on a 2° × 2° grid derived from ICOADS SST version 3 (Huang et al., 2017). ERSST 5 is spatially complete, as coverage gaps are filled with statistical methods. The monthly analysis extends from January 1854 to the present, but because of sparse data, there is damping of the analyzed signal before 1880. ERSST is suitable for long-term global and basin-wide studies. Local and short-term variations are smoothed.

The HadISST is a combination of monthly globally complete fields of SST and sea ice concentration for 1871 to present (Rayner et al., 2003). HadISST uses reduced space optimal interpolation applied to SSTs from the Marine Data Bank (mainly ship tracks) and ICOADS through 1981 and a blend of in situ and adjusted satellite-derived SSTs for 1982 onward. A bias correction was applied to SSTs for 1871–1941; that is, there is no correction of the World War II bias, as it does not account for changes in SST measurement practices post-1941. HadISST is a global, spatially complete data set of SST.

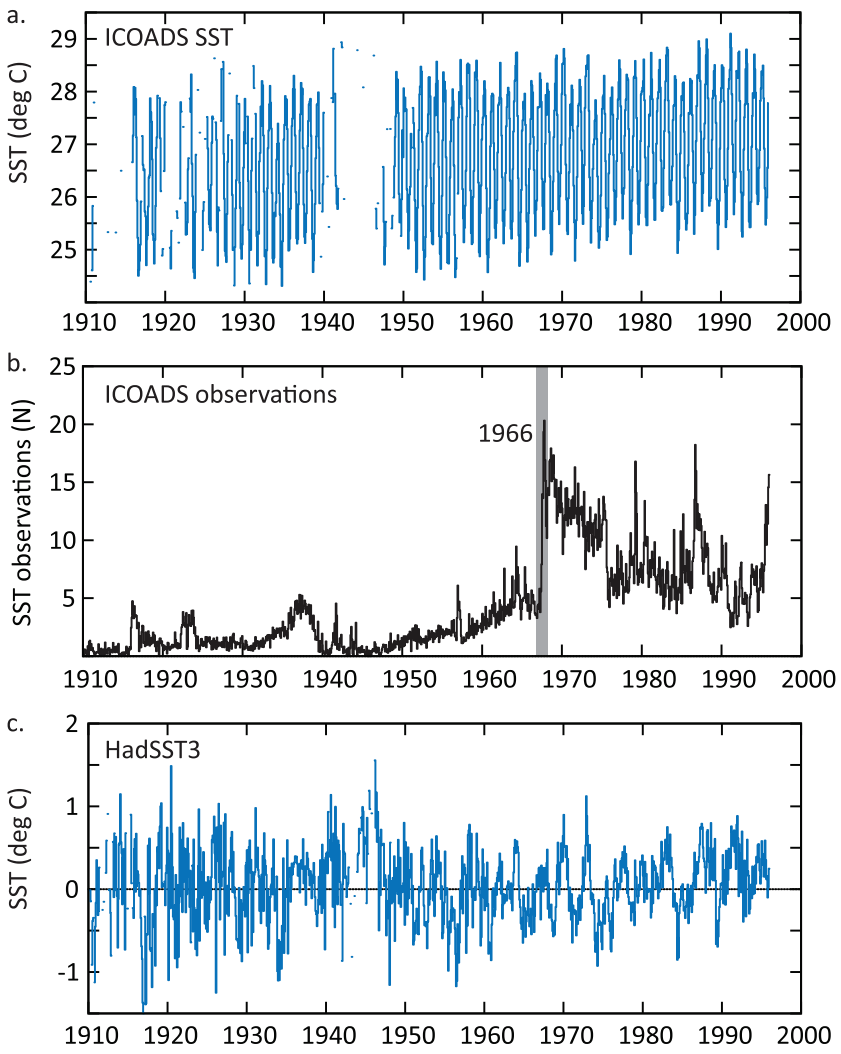

Figure 3. Historical surface temperature observations in the SW tropical Indian Ocean. (a) ICOADS data averaged over the region 55–80°E, 5–20°S. The number of observations in this region drops markedly in 1966, to fewer than five observations per month (b). During World War II, observations are lacking. (c) HadSST3 data (monthly anomalies) averaged over the region 55–80°E, 5–20°S.

3. Methods

3.1. Sampling and Analytical Procedures

The La Reunion core published by Pfeiffer et al. (2004) contained monthly (1976–1995) and bimonthly resolved $\delta^{18}O$ data (1832–1995), sampled parallel to the maximum axis of growth (Figure S4). Samples were taken along discrete spots every 1 mm with an automated milling device (Figure S5). For the bimonthly resolved $\delta^{18}O$ record, every second sample was analyzed. The core was resampled for Sr/Ca analysis by hand. Samples were taken at 1 mm intervals, next to the $\delta^{18}O$ drill holes (Figure S5). Samples for trace element analysis were collected from the coral slabs using a low-speed microdrill with a 0.5 mm diameter drill bit.

To assess the preservation of the La Reunion core samples were chosen for SEM and XRD analysis based on the X-ray images. The powder-XRD diffractometer at Rheinisch-Westfaelische Technische Hochschule Aachen University was calibrated to detect and quantify very low calcite contents above ~0.2 % following the method of Smodej et al. (2015). No calcite was detected by powder-X-ray diffraction (XRD) analysis. Scanning electron microscopy (SEM) images are used to screen the coral for aragonite cements. The upper section of the La Reunion core is very well preserved, and SEM images show pristine, smooth surfaces of unaltered coral skeleton. Pervasive thin aragonite cements start to occur at the base of slab 377 (~1900–

1910), while in the upper section (transect 1 and 2) of this slab SEM images show a pristine coral skeleton (Figure S5). Coral Sr/Ca and Mg/Ca from the base of slab 377 show effects of diagenesis in the form of a poorly defined seasonal cycle. We therefore limit the analysis of the La Reunion core to the end of Transect 1 on slab 377, which corresponds to the year 1913 AD.

Trace elements were measured in an inductively coupled plasma atomic emission spectrophotometer at the Geological Institute of the University of Kiel following a combination of the techniques described in detail by Schrag (1999) and de Villiers et al. (2002). Approximately 0.5 mg of coral powder was dissolved in 1.00 ml 0.2 M HNO3. Prior to analysis, the solution was diluted with 0.2 M HNO3 to a final concentration of ~8ppm Ca. Sr and Ca intensity lines used are 407 and 317 nm, respectively. The intensities of Sr and Ca were then converted into Sr and Ca ratios in mmol/mol. An in-house coral reference standard (Mayotte) was measured after every six samples and was used for drift correction of the measured Sr/Ca ratios. Analytical precision on Sr/Ca determinations is 0.15% relative standard deviation (RSD) or 0.01 mmol/mol (1σ) (Mayotte, $n = 989$). The reproducibility of Sr/Ca ratios from multiple measurements on the same day and on consecutive days is about 0.09% RSD (1σ).

The age model was developed by assigning 15 August to each annual Sr/Ca [$\delta^{18}O$] maximum. We then linearly interpolated between these anchor points to obtain monthly (bimonthly) time series of coral Sr/Ca [$\delta^{18}O$]. This creates a noncumulative error of 1 to 2 months in any year (Charles et al., 1997). To calculate $\delta^{18}O_{sw}$, coral Sr/Ca was interpolated to bimonthly resolution to match the temporal resolution of coral $\delta^{18}O$.

3.2. $\delta^{18}O_{sw}$ Calculation and Uncertainty Estimates

$\delta^{18}O_{sw}$ values were calculated from the paired proxy records following Cahyarini et al. (2008). In a first step, coral Sr/Ca and $\delta^{18}O$ were centered by removing their mean, and in a second step, relative variations of $\delta^{18}O_{sw}$ were calculated by subtracting the temperature component (inferred from the centered coral Sr/Ca record) from the centered coral $\delta^{18}O$ record (equation (1)):

$$\delta^{18}\mathrm{Osw} = \left(\delta^{18}\mathrm{Ocoral} - \overline{\delta^{18}\mathrm{Ocoral}}\right) - \frac{\gamma_1}{\beta_1}\left(\mathrm{Sr/Ca} - \overline{\mathrm{Sr/Ca}}\right)$$

where δ^{18}Ocoral is measured coral $\delta^{18}O$, $\overline{\delta^{18}\mathrm{Ocoral}}$ is the mean value of measured coral $\delta^{18}O$, Sr/Ca is measured coral Sr/Ca, $\overline{\mathrm{Sr/Ca}}$ is the mean of measured Sr/Ca, $y_1$is the regression slope of coral $\delta^{18}O$ versus SST, and β_1 is the regression slope of coral Sr/Ca versus SST. The error of $\delta^{18}O_{sw}$ is calculated using equation (2):

$$\sigma^2{}_{\delta\mathrm{sw}} = \sigma^2{}_{\delta c} + \left(\frac{\gamma_1}{\beta_1}\right)^2 \sigma^2{}_{\mathrm{Sr/Ca}}$$

where $\sigma_{\delta sw}$ is the error of reconstructed $\delta^{18}O_{sw}$, $\sigma_{\delta c}$ is the error of measured $\delta^{18}O_{coral}$, $\sigma_{Sr/Ca}$ is the error of measured Sr/Ca, and y_1 and β_1 are the slopes of the linear regression of $\delta^{18}O$ versus SST and Sr/Ca versus SST, respectively (see Cahyarini et al., 2008, for discussion).

The analytical error is ±0.06‰ for coral $\delta^{18}O$ (Pfeiffer et al., 2004) and ±0.01 mmol/mol for coral Sr/Ca. Published slope values for the $\delta^{18}O$-SST relationship range from −0.18 to −0.22‰ per 1 °C (mean: −0.2‰ per 1 °C; Juillet-Leclerc & Schmidt, 2001). The Sr/Ca-SST relationship ranges from −0.04 to −0.08 mmol/mol per 1 °C (mean: −0.06 mmol/mol per 1 °C; Corrège, 2006). Combining the analytical errors with the published mean slope values results in an error of ±0.069‰ (1σ) for bimonthly $\delta^{18}O_{sw}$ anomaly values. Combining the analytical uncertainties with the maximum and minimum values of the published proxy-SST slopes (so that maximum errors for $\delta^{18}O_{sw}$ are obtained, that is, y_1 = −0.22‰ per 1 °C and β_1 = −0.04 mmol/mol per 1 °C) results in an uncertainty of ±0.081‰ (1σ).

The uncertainties of the bimonthly Sr/Ca ($\delta^{18}O$) values are independent, as the analytical errors of each coral $\delta^{18}O$ and Sr/Ca determination are independent. Therefore, the uncertainties for annual mean Sr/Ca ($\delta^{18}O$) values reduce according to equation (3):

$$\sigma_{\mathrm{Total}} = \sqrt{\left(\sigma^2/_N\right)}$$

where N is the number of independent Sr/Ca ($\delta^{18}O$) determinations and σ_{Total} the uncertainty of each

annual mean estimate computed from six bimonthly values. The uncertainty of annual mean Sr/Ca ($\delta^{18}O$) is ±0.004 mmol/mol (±0.024‰). Inserting these values in equation 2, the analytical uncertainty of annual mean $\delta^{18}O_{sw}$ is ±0.033‰ (1σ).

3.3. Statistical Analysis

Linear ordinary least squares (OLS) regression analysis were performed with the PAleontological STatistics (PAST) software package (Hammer et al., 2001). The software estimates 95% bootstrapped confidence intervals (N = 1,999). The residuals of all linear regression models shown in this paper were randomly scattered around zero, indicating that OLS regression provides robust estimates. Wavelet Power spectra were also computed with the PAST software package (Figure S6).

Running correlations were computed using the Koninklijk Nederlands Meteorologisch Instituut (KNMI) Climate Explorer (http://climexp.knmi.nl; van Oldenborgh & Burgers, 2005). Ninety five percent confidence intervals are estimated with a 1,000-sample Monte Carlo.

4. Results

4.1. Data

Figure 4 shows the new monthly coral Sr/Ca time series and bimonthly $\delta^{18}O$ time series published in Pfeiffer et al. (2004) for the time period from 1913 to 1995. The bimonthly $\delta^{18}O_{sw}$ anomaly record calculated from the centered (i.e., mean removed) bimonthly coral Sr/Ca and $\delta^{18}O$ time series is also shown. Coral Sr/Ca and $\delta^{18}O$ show large seasonal cycles reflecting the large temperature seasonality of >4.5 °C at La Reunion Island (Figures 4 and S6). Coral Sr/Ca shows significant decadal to interdecadal variability in the midtwentieth century and multidecadal variability, while coral $\delta^{18}O$ shows interannual and multidecadal variability (Figures 4 and S6). Bimonthly coral $\delta^{18}O_{sw}$ shows a poorly defined seasonal cycle and significant interannual, interdecadal, and multidecadal variability, reflecting the contribution of both coral Sr/Ca and $\delta^{18}O$ (Figures 4 and S6).

4.2. Calibration

The monthly coral Sr/Ca data are calibrated with satellite SST (OI SST, 1° × 1° grid; Reynolds et al., 2002), which extends back to 1982 (Figure 5). The correlation is high ($r = -0.81$, $N = 164$, $p < 0.01$) due to the strong seasonal cycle in both data sets, and the Sr/Ca-SST slope (−0.04 mmol/mol per 1 °C) is consistent with published estimates that range from −0.04 to −0.08 mmol/mol per 1 °C (Corrège, 2006). Given the large number of data gaps in historical SST in the 5° × 5° grid including La Reunion, we evaluated the annual mean Sr/Ca record with HadSST3 data averaged over a larger region in the SW tropical Indian Ocean (55–80°E, 5–20°S) (Figure 6). Running correlation analysis (9-year sliding windows) shows that coral Sr/Ca correlates with regional SST back to 1966. The correlation breaks down with the drop in the number of observations in the SW Indian Ocean prior to 1966 (Figure 3b). A linear regression of annual mean coral Sr/Ca versus HadSST3 for the time period 1966–1995 shows a high correlation ($r = -0.69$, $N = 29$, $p < 0.01$) and a slope value of −0.068 (95% confidence interval (CI): −0.09, −0.45) mmol/mol per 1 °C. This is again consistent with published estimates summarized in Corrège (2006) and justifies to use the mean and spread of the Sr/Ca-SST slope from that study for the temperature conversion of the La Reunion Sr/Ca record.

Monthly (1976–1995) and bimonthly coral $\delta^{18}O$ variations show a pronounced seasonal cycle (Figure S6) and a high correlation with grid temperature (Pfeiffer et al., 2004). The slopes of the monthly $\delta^{18}O$/temperature relationships are consistent with published estimates of the $\delta^{18}O$-SST relationship (Pfeiffer et al., 2004). On an annual mean scale, however, there is no significant correlation between coral $\delta^{18}O$ and SST, regardless of the SST product or time period chosen for calibration (Pfeiffer et al., 2004). Figure 6 shows a running correlation of annual mean coral $\delta^{18}O$ versus HadSST3 (55–80°E, 5–20°S). While coral Sr/Ca correlates with HadSST3 back to 1966, coral $\delta^{18}O$ does not show any significant relationship with historical SST before or after 1966. A linear regression of annual mean coral $\delta^{18}O$ and HadSST3 for the time period 1966–1995 yields a slope value that is not significantly different from zero (−0.02‰ per 1 °C; 95% CI: −0.12 to 0.1‰ per 1 °C, $N = 29$, $p > 0.5$) (Figure 6). Tables S1 and S2 summarize the Sr/Ca and $\delta^{18}O$-SST relationships for seasonal data (using seasonal minima/maxima) and annual means.

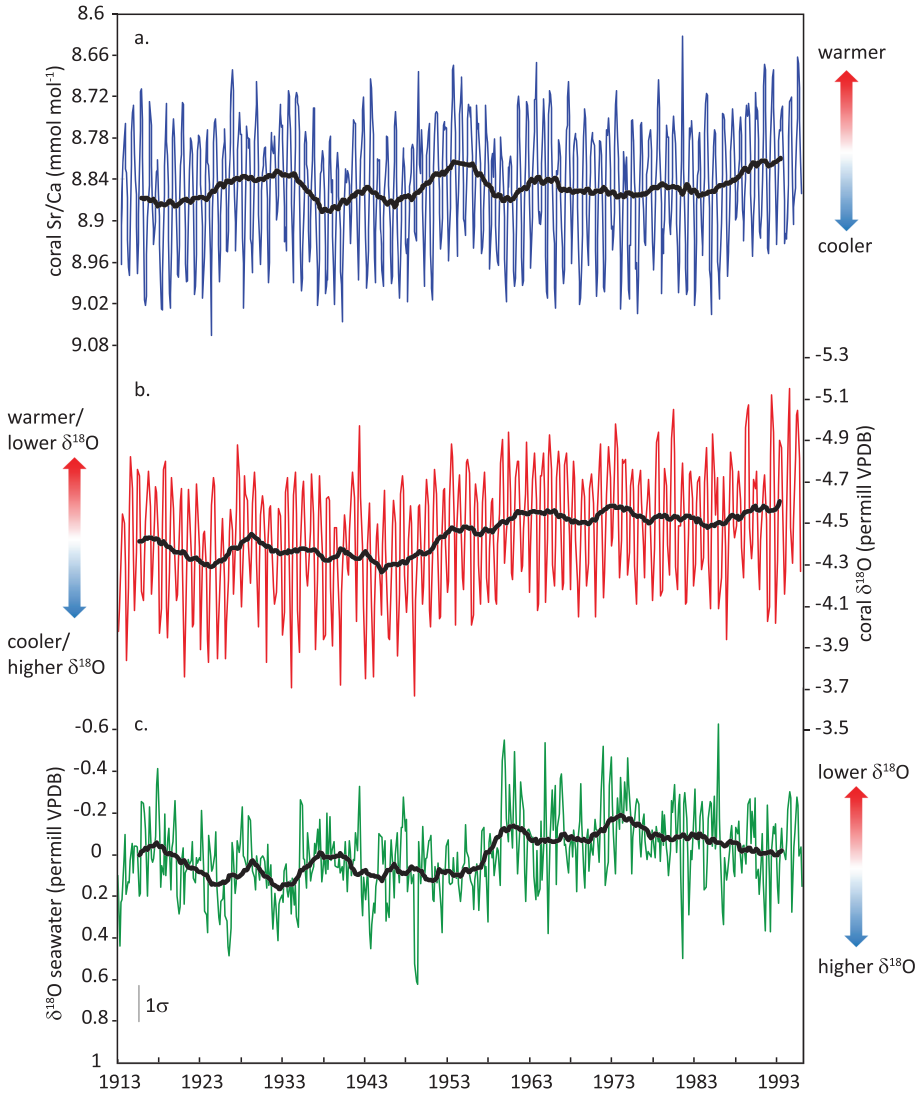

Figure 4. Coral geochemical records. (a) Monthly coral Sr/Ca (blue), (b) bimonthly coral δ^{18}O (red), and (c) bimonthly coral δ^{18}O seawater (green) computed by subtracting the temperature component inferred from bimonthly Sr/Ca and δ^{18}O. Black thick lines are 31-point moving averages.

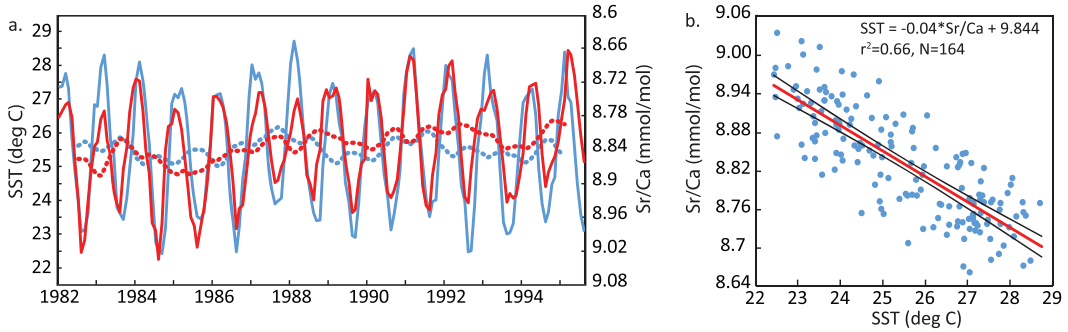

Figure 5. Calibration of monthly coral Sr/Ca. (a) Time series of monthly OI SST (blue lines; grid centered at 55°E, 21°S; Reynolds et al., 2002) and monthly coral Sr/Ca data measured at La Reunion (red lines) for the time period 1982–1995. Thick dashed lines are 13-point moving averages of monthly data. (b) Linear OLS regression of monthly coral Sr/Ca versus OI SST with 95% confidence levels. See text for discussion.

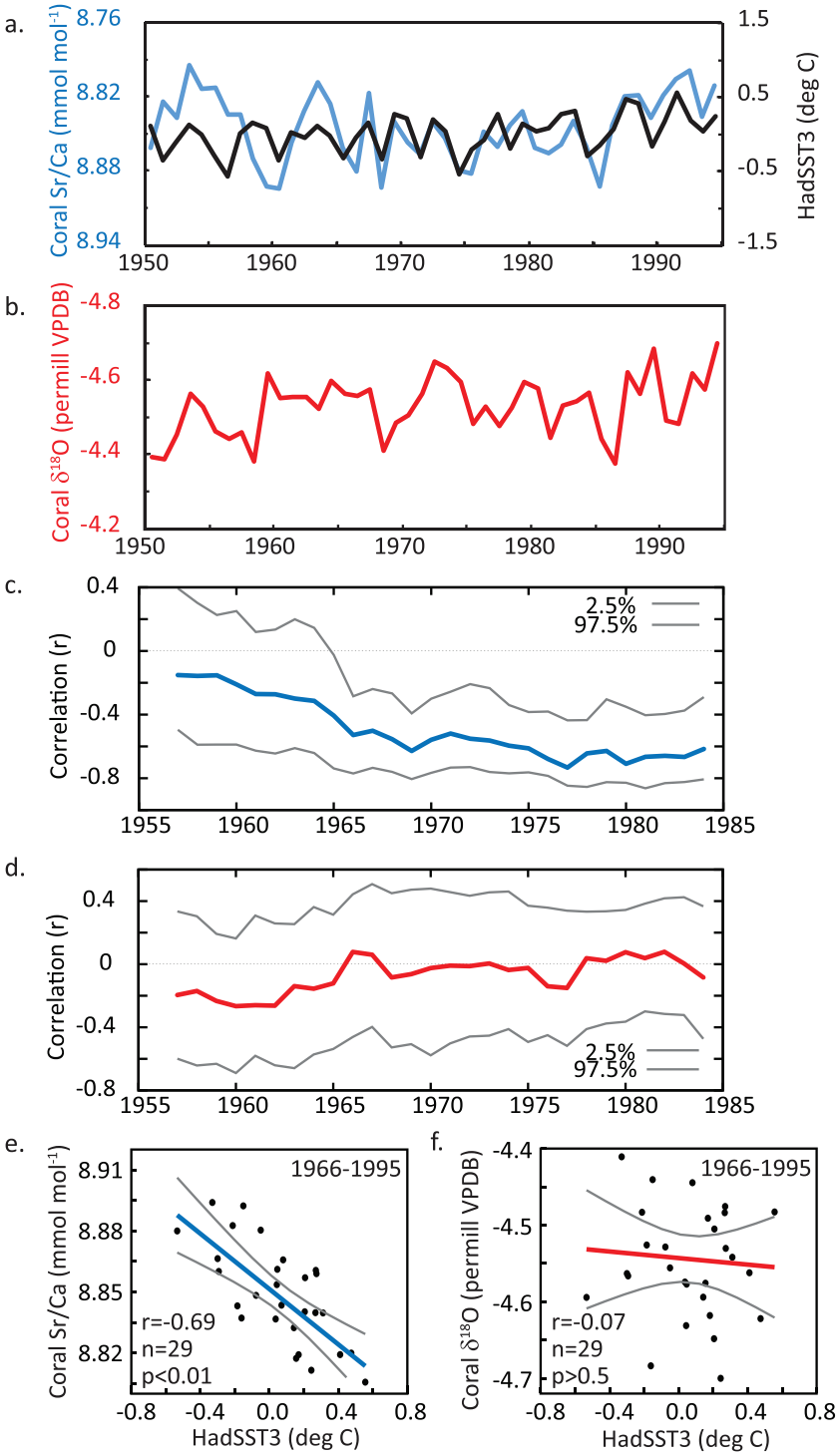

Figure 6. Correlation of annual mean coral proxies vs. historical SST. (a) Time series of coral Sr/Ca and annual mean HadSST3 averaged over the SW Indian Ocean (55–80°E, 5–20°S). (b) Annual mean coral $\delta^{18}O$. (c) Running correlation with 9-year sliding window of coral Sr/Ca versus HadSST3. (d) Running correlation with 9-year sliding window of coral $\delta^{18}O$ versus HadSST3. (e) Linear OLS regression of coral Sr/Ca versus HadSST3 for the time period 1966–1995. The correlation is high and the slope value is −0.068 mmol/mol per 1 °C (95% CI: −0.09, −0.045). (f) Linear OLS regression of coral $\delta^{18}O$ versus SST for the time period 1966–1995. The correlation is not significant ($p > 0.5$) and the slope of the coral $\delta^{18}O$-SST regression is not significantly different from zero (−0.02‰ per 1 °C; 95% CI: −0.12, 0.1).

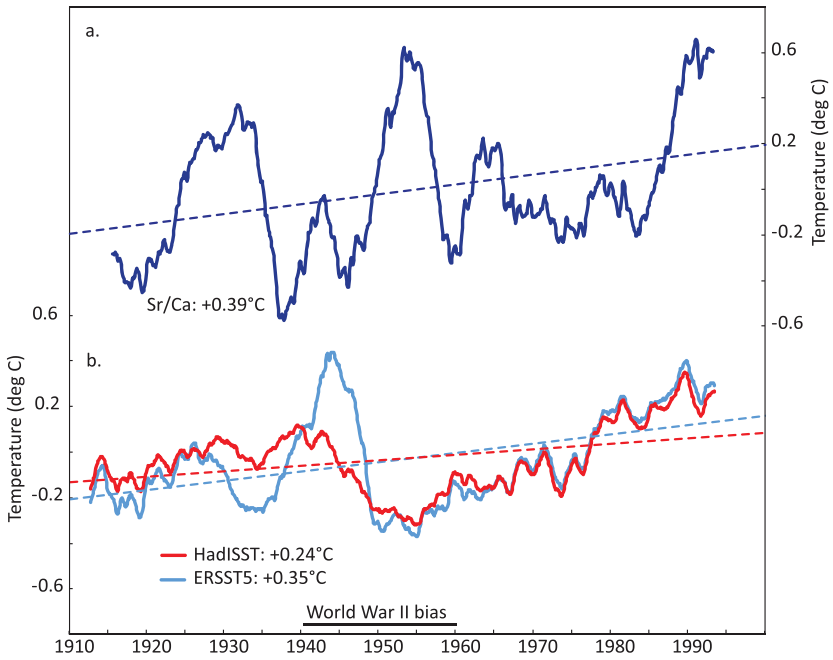

Figure 7. Sea surface temperature trends. Warming rates estimated from coral Sr/Ca are compared with warming rates of SST observations averaged over the SW Indian Ocean (55–80°E, 5–20°S). All time series are 61-point moving averages of monthly anomalies. (a) coral Sr/Ca (centered and converted to temperature using −0.06 mmol/mol per 1 °C). Sr/Ca shows a warming of 0.39 °C since 1913 (95% CI: 0.29–0.60 °C). Pronounced decadal to interdecadal shifts occur prior to 1960 and again after the 1980s. (b) Instrumental SSTs show warming rates ranging from 0.24 °C (HadISST, red lines) to 0.35 °C (ERSST5, blue lines). Decadal to interdecadal variability is of lower magnitude, except between the 1940s and 1960s. Note that the uncertainties of instrumental SST are largest in this time period (World War II bias).

4.3. Temperature Trends

Figure 7 compares long-term and low-frequency temperature variations inferred from La Reunion coral Sr/Ca with ERSST5 and HadISST data averaged over the SW tropical Indian Ocean (55–80°E, 5–20°S). Since 1913, coral Sr/Ca shows a long-term decrease of −0.024 mmol/mol (95% Cl: −0.033 to −0.014 mmol/mol). This translates into a long-term temperature trend of +0.39 °C (95% CI: +0.24 to +0.55 °C), assuming a coral Sr/Ca-temperature relationship of −0.06 mmol/mol per 1 °C (Table 1). The minimum warming rate indicated by coral Sr/Ca is 0.18 °C since 1913 (estimated by converting the lower 95% CI of the long term trend in coral Sr/Ca to temperature using −0.08 mmol/mol per 1 °C; see also Table 1). Interdecadal warm anomalies are seen between 1925–1935, 1950–1957 and from the late 1980s–1995.

Table 1
Warming Rates of the SW Indian Ocean Estimated From Coral Proxies and Instrumental Data

Dataset	Proxy	95% Cl	°C	95% Cl	Minimum warming
Sr/Ca	−0.024[a]	(−0.014/−0.033)[a]	0.39	(0.24/0.55)	0.18
$\delta^{18}O$	−0.26[b]	(−0.23/−0.29)[b]	1.29	(1.15/1.45)	1.05
ERSST5 °C			0.35	(0.28/0.44)	
HadISST °C			0.24	(0.18/0.30)	

Note. Linear trends (OLS regression) are calculated from monthly anomalies of coral Sr/Ca and $\delta^{18}O$ and converted to warming rates (in °C) using –0.06 mmol/mol per 1 °C (Sr/Ca) and –0.2‰ per 1 °C ($\delta^{18}O$. Results are compared with linear trends of historical SST data averaged over the SW Indian Ocean (55–80°E, 5–20°S; 1966–1995). Minimum warming rates are estimated from the coral proxies by converting the lower 95% confidence interval of the linear trend to SST units using a proxy-SST relationship of –0.22‰ per 1 °C for $\delta^{18}O$ and –0.08 mmol/mol per 1 °C for Sr/Ca.
[a]The unit is millimoles per mole.
[b]bThe unit is permil. See text for discussion.

ERRSST5 indicates a warming of +0.35 °C (95% Cl: +0.28 to +0.44 °C) in the SW tropical Indian Ocean. A prominent decadal to interdecadal warm anomaly is centered at 1945, followed by a slight cooling in the 1950s to 1960s. The 1945 warm anomaly is much smaller in the coral Sr/Ca record. HadISST shows slightly lower warming rates of +0.24 °C (95% Cl: +0.18 to +0.30 °C).

Over the time period from 1913 to 1995, coral $\delta^{18}O$ shows a decrease of −0.26‰ (95% Cl: −0.23 to −0.29‰), which would indicate a warming of +1.29 °C when assuming a coral $\delta^{18}O$-SST relationship of −0.2‰ per 1 °C (Juillet-Leclerc & Schmidt, 2001; Table 1). Minimum warming rates are estimated by converting the lower 95% Cl of the coral $\delta^{18}O$ trend (−0.23‰) to SST using a $\delta^{18}O$-SST relationship of −0.22‰ per 1 °C. This would result in a warming of 1.05 °C since 1913, which is three times larger than the temperature rise indicated by ERSST5 (Table 1).

4.4. $\delta^{18}O$ Seawater

Annual mean $\delta^{18}O_{sw}$ is calculated by subtracting the temperature component from coral $\delta^{18}O$ following Cahyarini et al. (2008). The temperature component is (I) estimated from annual mean coral Sr/Ca and (II) taken from annual mean ERSST5 and HadISST averaged over 55–80°E and 5–20°S (Figure S7). All time series are centered by removing their mean. Figure 9 compares annual mean and decadal-multidecadal variations (9-point moving averages) of the three $\delta^{18}O_{sw}$ reconstructions. The reconstructions are linearly correlated ($r = 0.67$ for the coral Sr/Ca-based reconstruction versus ERSST5 and $r = 0.72$ for the coral Sr/Ca-based reconstruction versus HadISST, $N = 82$, $p < 0.01$) and show multidecadal changes of comparable magnitudes. Note that the time scale of these $\delta^{18}O_{sw}$ variations is long compared to the time span covered by the proxy record. A significant shift toward lower $\delta^{18}O_{sw}$ occurs in the midtwentieth century. However, the timing of this shift varies from ~1945/1946 ($\delta^{18}O_{sw}$ estimated with instrumental SST) to the late 1950s ($\delta^{18}O_{sw}$ estimated with coral Sr/Ca), that is, by more than 10 years. For the Sr/Ca-based reconstruction, mean $\delta^{18}O_{sw}$ averaged over the 1920–1940 period is 0.13‰, compared to −0.06‰ during 1958–1978 (mean values are significantly different at the 99% confidence level based on a two-sided student's t test). This amounts to a freshening of 0.19‰. Mean $\delta^{18}O_{sw}$ estimated using ERSST5 [HadISST] shows a significant freshening of 0.17 [0.19] ‰ between 1920–1940 and 1957–1978, that is, the same magnitude.

5. Discusssion

5.1. La Reunion Coral Sr/Ca and $\delta^{18}O$

Pfeiffer et al. (2004) suggested that coral $\delta^{18}O$ measured at La Reunion primarily showed variations of $\delta^{18}O_{sw}$ and SSS at time scales longer than the seasonal cycle. However, this interpretation was solely based on the lack of correlation of mean annual coral $\delta^{18}O$ with historical SST data products. These historical SST data sets are produced from sparse data and averaged over large spatial scales, and they are not meant to indicate reef-scale SST variations that would be recorded by a coral geochemical record (Huang et al., 2017; Kennedy et al., 2011a, 2011b; Rayner et al., 2003). This uncertainty has limited the use of the Reunion coral isotopic record for large-scale climate reconstructions. The new coral Sr/Ca data measured on a parallel transect to the coral $\delta^{18}O$ record do show a significant correlation with historical SST in the SW tropical Indian Ocean back to 1966, when instrumental coverage is good. Also, the slope of the coral Sr/Ca-temperature relationship is consistent with published estimates. This confirms that the Reunion coral is from a site where large-scale SST variations are portrayed by reef-scale SST. In addition, this supports the previous interpretation that Reunion coral $\delta^{18}O$ does show $\delta^{18}O_{sw}$ and SSS rather than local water temperature (Pfeiffer et al., 2004). The breakdown of the correlation between coral Sr/Ca and historical SST prior to 1966 likely reflects the drop in the number of observations in the ICOADS database. Previous work in the central Indian Ocean has shown that the proxy-SST correlation is higher in times when a large number of SST observations is available (Pfeiffer et al., 2017). However, the Reunion coral Sr/Ca record derives from one single coral core and lacks replication. Single-core reconstructions typically also have lower correlations with grid SST than composite reconstructions from multiple cores (e.g., DeLong et al., 2013; Pfeiffer et al., 2009; Pfeiffer et al., 2017). Moreover, single-core Sr/Ca records may at times deviate from large-scale SST for a number of reasons, and not all of them are currently understood (e.g., Hendy et al., 2007; Pfeiffer et al., 2009; Grove, Kasper, et al., 2013; Zinke et al., 2016; Sayani et al., 2019). Deviations probably result from a combination of factors, including reef-scale temperatures, vital effects, secondary alterations, and changes in coral

growth and calcification rates. SEM and XRD analysis show that the Reunion core is free of secondary alterations between 1913 and 1995. However, due to its high relief, La Reunion has pronounced windward/leeward effects, which may influence reef-scale SST (Figure S1) although time-dependent deviations between east and west coast SST are largest on a subseasonal time scale (not shown).

5.2. Warming of the SW Indian Ocean

Taking into account the regression uncertainty and the range of published Sr/Ca-SST relationships, the long-term warming trend inferred from coral Sr/Ca is consistent with the warming indicated by historical SST data averaged over the SW Indian Ocean. However, the pattern of decadal and interdecadal variability differs, with coral Sr/Ca showing warm intervals between 1925–1935, 1950–1957 and from the late 1980s–1995, while historical SST data show a prominent warm anomaly centered at 1945 followed by a slight cooling from 1950–1960. In this time interval, the uncertainties of instrumental SST are large due to sparse observations during World War II and changes in the measurement procedures of voluntary observing ships (Kennedy et al., 2011a, 2011b; Pfeiffer et al., 2017; Thompson et al., 2008). In the SW tropical Indian Ocean, ICOADS SST has large data gaps between 1940 and 1950 (Figure 3). Owing to a switch in the technique of measuring SSTs during [after] World War II to predominantly engine room intake [bucket] measurements, mean SSTs between 1940 and 1945 [1945–1960] are biased warm [cool]. This pattern is seen in the historical SST data from the SW Indian Ocean and suggests that the data may be biased, as seen also in the tropical Indian Ocean (Pfeiffer et al., 2017). Replication of the Reunion coral Sr/Ca record is needed to better assess decadal to interdecadal SST variability in the SW tropical Indian Ocean.

The long-term decrease of coral $\delta^{18}O$ in the 1913–1995 period is two to three times as large as the warming indicated by coral Sr/Ca and historical SST products (Table 1, "minimum warming"). This suggests a significant freshening trend in the SW tropical Indian Ocean since 1913 that contributes to the decrease in coral $\delta^{18}O$. This is an important observation, as the Reunion coral $\delta^{18}O$ record has been included in the PAGES 2k Indian Ocean temperature reconstruction (Tierney et al., 2015), because it appeared to correlate with large-scale Indian Ocean SST in the target area of this study (20°N–15°S, 40°–100°E). However, this correlation results from the long-term linear trends present in both data sets, that is, the trend toward lower $\delta^{18}O$ of the Reunion isotope record inflates its correlation with tropical Indian Ocean SSTs, which show a pronounced twentieth century warming trend (e.g., Pfeiffer et al., 2017; Roxy et al., 2014). Removing the linear trends reduces this correlation to zero (not shown), suggesting that it is a spurious result.

The current reanalysis of the La Reunion core suggests small but pervasive amounts of aragonite cements typical for marine diagenesis prior to 1913 AD, which appears to affect the coral Sr/Ca ratios. Aragonite cements are typical for early marine diagenesis and cause "cold anomalies" in coral Sr/Ca and $\delta^{18}O$ (e.g., Hendy et al., 2007; Sayani et al., 2011). Coral Sr/Ca is typically more sensitive to diagenetic changes than coral $\delta^{18}O$ (Sayani et al., 2011), so this problem was not detected in Pfeiffer et al. (2004). Coral $\delta^{18}O$ displays regular seasonal cycles back to 1832 AD. However, diagenesis may also affect the long-term trend of coral $\delta^{18}O$, so the La Reunion $\delta^{18}O$ data prior to 1913 may be biased toward higher values. Note that the La Reunion coral $\delta^{18}O$ record shows a strong trend toward lower $\delta^{18}O$ of approximately −0.7‰ since 1832 (Pfeiffer et al., 2004). This would indicate a warming of 3.5 °C (if entirely temperature related), or a freshening of >2.5 psu (based on $\delta^{18}O_{sw}$-SSS data of Srivastava et al., 2007). Both values exceed the range of interannual variability currently observed at La Reunion. It is therefore likely that the La Reunion coral $\delta^{18}O$ record inflates the cooling of the PAGES 2k tropical Indian Ocean temperature reconstruction between 1833 and 1842, as discussed in Tierney et al. (2015).

5.3. Seawater $\delta^{18}O$ and Salinity in the SW Indian Ocean

We have calculated three annual mean $\delta^{18}O_{sw}$ reconstructions from the La Reunion coral $\delta^{18}O$ data (Figure 8), one using coral Sr/Ca and two using SST data averaged over the SW tropical Indian Ocean from different historical SST products (ERSST5 and HadISST; Figure S7). Theoretically, the $\delta^{18}O_{sw}$ reconstruction using coral Sr/Ca should be the best one, as coral Sr/Ca should provide an accurate record of reef-scale SST. Grid SST from historical products are primarily estimated to capture large-scale temperature trends and to provide boundary conditions for climate model simulations (Huang et al., 2017; Kennedy et al., 2011a, 2011b; Rayner et al., 2003) and have a low spatial resolution. However, recent studies have suggested that processes other than SST may influence coral Sr/Ca on decadal and longer time scales (e.g., Grove,

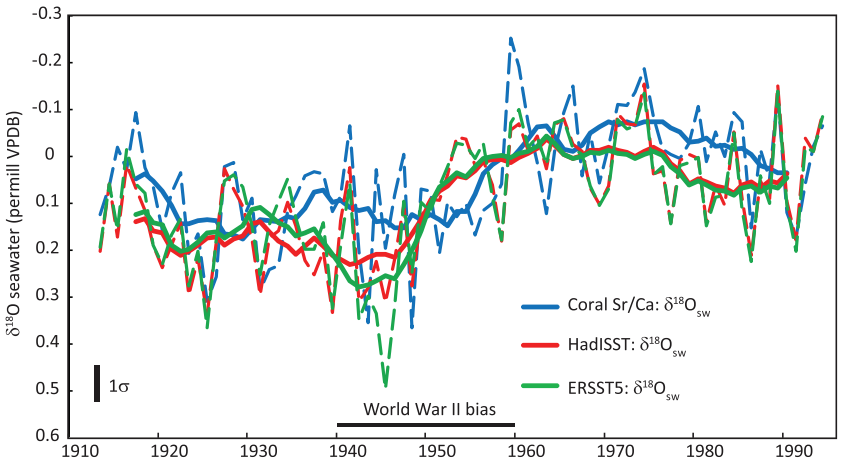

Figure 8. $\delta^{18}O$ seawater reconstrutions. Annual mean $\delta^{18}O$ seawater changes are estimated by subtracting the temperature component inferred from coral Sr/Ca (blue lines) and instrumental SST (HadISST: red lines; ERSST5: green lines) from measured coral $\delta^{18}O$. Thin dashed lines are annual means, centered to their mean. Solid thick lines are 9-point moving averages. Note that the magnitude of multidecadal $\delta^{18}O$ seawater variations computed using coral Sr/Ca is consistent with $\delta^{18}O$ seawater variations computed using instrumental SST. However, the timing of major shifts differs by more than 10 years.

Kasper, et al., 2013; Zinke et al., 2016). As the Reunion Sr/Ca record currently lacks replication with independent coral cores, we decided to compare the Sr/Ca-based $\delta^{18}O_{sw}$ reconstruction with the SST-based reconstructions to get some indication of its reliability. This does allow an evaluation of the $\delta^{18}O_{sw}$ reconstruction that extends beyond the error estimates calculated from the analytical uncertainties. (The latter are only valid if our assumptions regarding the coral proxies are correct, that is, when coral Sr/Ca is solely a temperature proxy and not systematically affected by factors other than temperature.)

All three $\delta^{18}O_{sw}$ reconstructions show a shift toward more depleted values in the middle of the twentieth century. The magnitude of this shift is consistent, ranging from of 0.17‰ to 0.19‰, depending on the data used to subtract the temperature component from coral $\delta^{18}O$. Srivastava et al. (2007) performed a combined analysis of stable oxygen isotopes ($\delta^{18}O$) and salinity of western Indian Ocean surface waters along a transect from India to Antarctica. For the Indian Ocean north of 44°S, the authors report a linear $\delta^{18}O_{sw}$–salinity relationship ($\delta^{18}O_{sw} = -0.27 \pm 0.03$*SSS) and a high correlation ($r^2 = 0.73$, $p \sim 0$). Using this relationship, the 0.19‰ decrease of $\delta^{18}O_{sw}$ from 1920–1940 to 1958–1978 would translate into a freshening of 0.7 (0.63–0.79) psu. (Note that the analytical error of coral $\delta^{18}O_{sw}$ estimated from Sr/Ca and $\delta^{18}O$ reduces to <0.01‰ for 21-year averages and has been neglected.) On interannual time scales, satellite data show SSS variations with comparable magnitudes (Figure 2); that is, the magnitude of the estimated freshening may be realistic.

However, the timing of the midtwentieth century shift in $\delta^{18}O_{sw}$ and SSS toward lower $\delta^{18}O$ and SSS values differs. Both grid-based reconstructions show a shift toward lower $\delta^{18}O$ and SSS around 1946. In contrast, the Sr/Ca-based reconstruction suggests that the timing of this shift occurs in the late 1950s, approximately 10 years later (Figure 8). This apparent offset is caused by the SST contribution that is subtracted from measured coral $\delta^{18}O$. Coral Sr/Ca shows warmer temperatures in the 1950s (Figure 7), and this translates into higher $\delta^{18}O_{sw}$ estimates during these years (Figure 8). The shift toward lower values therefore occurs in the late 1950s. Historical SST records show a warm anomaly from 1940 to 1945, followed by an abrupt drop from 1945 to 1950, a pattern resembling the so-called World War II bias that is an artifact of changes in the measurement procedures (e.g., Thompson et al., 2008). This bias would introduce an artifact in the LA Reunion $\delta^{18}O_{sw}$ and SSS reconstruction estimated with historical SSTs. A warm bias from 1940 to 1945 would result in higher $\delta^{18}O_{sw}$ estimates, while a cool bias after 1945 would result in lower estimates. Interestingly, this pattern is observed in both ERSST5 and HadISST, although attempts have been made to correct the World War II bias in ERSST5, but not in HadISST (Huang et al., 2017; Rayner et al., 2003). Pfeiffer et al. (2017) have shown that the World War II bias is a prominent feature in tropical Indian Ocean SSTs.

The timing of the $\delta^{18}O_{sw}$ shift is important, because it affects the interpretation of the $\delta^{18}O_{sw}$ reconstruction, in particular with regard to potential teleconnections to large-scale climate modes. Pfeiffer et al. (2004) suggested that $\delta^{18}O_{sw}$ variations reflect the transport of the SEC, with lower values at La Reunion being caused by a stronger SEC, which carries fresh water from the Indonesian Throughflow (ITF) and the ITCZ toward the western Indian Ocean (Han & McCreary, 2001; Schott et al., 2009). Multidecadal variations in the transport of the south Indian Ocean gyre have been described in a number of studies, and these have been attributed to changes in the wind field over the southern Indian Ocean as well as remote influences from the Pacific Ocean (see Han et al., 2014 for a review). The Pacific influences the Indian Ocean via the ITF and via the atmospheric bridge over the maritime continent. Robust large-scale teleconnections between the Indian and Pacific Ocean are seen on interannual time scales (Han et al., 2014).

Pfeiffer et al. (2004) suggested that multidecadal variations of the La Reunion $\delta^{18}O_{sw}$ record are also driven by Pacific variability and reflect phase changes of the Pacific Decadal Oscillation (PDO). This interpretation is based on the out-of-phase relationship of coral $\delta^{18}O$ with historical SST that would translate into $\delta^{18}O_{sw}$ changes that coincide with phase changes of the PDO (i.e., the shift toward its negative phase in 1947 and the shift toward its positive phase in 1976, although the latter is weaker; see Pfeiffer et al., 2004). The negative [positive] phase of the PDO would cause an increase [decrease] in the transport of the ITF and lower [higher] $\delta^{18}O_{sw}$ and SSS along the path of the SEC. A number of studies now support this interpretation. For example, the ITF was shown to respond to the 1975 phase change of the PDO with a reduction in water mass transport (Wainwright et al., 2008), and coral luminescence records from the SW Indian Ocean show a PDO signature in regional rainfall (Grove, Zinke, et al., 2013). Moreover, Hennekam et al. (2018) showed that variations of the PDO appear to influence Indian Ocean $\delta^{18}O_{sw}$ and SSS via the ITF, based on a 200-year coral record from Cocos (Keeling). Cocos (Keeling) is located in the eastern Indian Ocean, within the path of the SEC and close to the ITF exit passages.

The new coral Sr/Ca data from the La Reunion core, however, suggest that the midtwentieth century shift in $\delta^{18}O_{sw}$ in the SW Indian Ocean occurs more than 10 years after the phase change of the PDO. $\delta^{18}O_{sw}$ reconstructions based on historical SST data, in contrast, would support a link with the PDO, as they show a mid-century shift toward more enriched $\delta^{18}O_{sw}$ around 1947, which coincides with the shift of the PDO from its positive to negative phase. However, these results depend on the uncertain SST data during and after World War II and could reflect the warm [cool] bias before [after] 1945 (Thompson et al., 2008). There is some indication in modeling studies that the atmospheric teleconnection between the Pacific and SW Indian Ocean breaks down on multidecadal time scales (Nidheesh et al., 2013), suggesting that the relationship between the Indian Ocean and Pacific varies in different decades. The Indian Ocean subtropical gyre responds to changes in the SE trades winds over the central Indian Ocean, which modulate the transport of the SEC (Zhuang et al., 2013). However, the magnitude of $\delta^{18}O_{sw}$ and SSS changes inferred from the La Reunion coral are difficult to explain without the ITF that advects of low salinity water from the maritime continent (Kuhnert et al., 2014). This suggests that internal processes in the Indian Ocean may modulate the meridional extend of the SEC. Note that La Reunion lies at the southern margin of the SEC (Figure 1).

5.4. Large-Scale Temperature Reconstruction in the SW Tropical Indian Ocean

Long temperature reconstructions based on coral Sr/Ca from the SW tropical Indian Ocean are still scarce, and some of the existing records are problematic because of apparent nontemperature effects, most likely related to coral growth patterns and calcification (Grove, Kasper, et al., 2013; Zinke et al., 2016). Another potentially confounding effect is reef-scale or site-specific temperature variations not recorded in grid-scale historical temperature products. These likely arise from the complex background climate in the SW tropical to subtropical Indian Ocean (Figures 1 and S1) and include windward/leeward effects (Pfeiffer et al., 2004), other reef-scale temperature effects (Zhang et al., 2013), and mixing of water masses via eddies (Zhuang et al., 2013; Figure 1). To date, only one long coral Sr/Ca record has been published from the SW Indian Ocean that shows a significant relationship with grid SST (Zinke et al., 2016). The core derives from Rodrigues Island (63°E, 19°S) and extends back to 1945. We have computed a composite annual mean coral Sr/Ca record as the arithmetic mean of the La Reunion and Rodrigues record (Figure 9). This simple (unweighted) average was chosen because the sparse historical SST data in the SW Indian Ocean precludes the estimation of differences in the SST variance at Rodrigues and La Reunion. The two coral records have been centered by removing their mean and converted to SST units using a coral Sr/Ca temperature

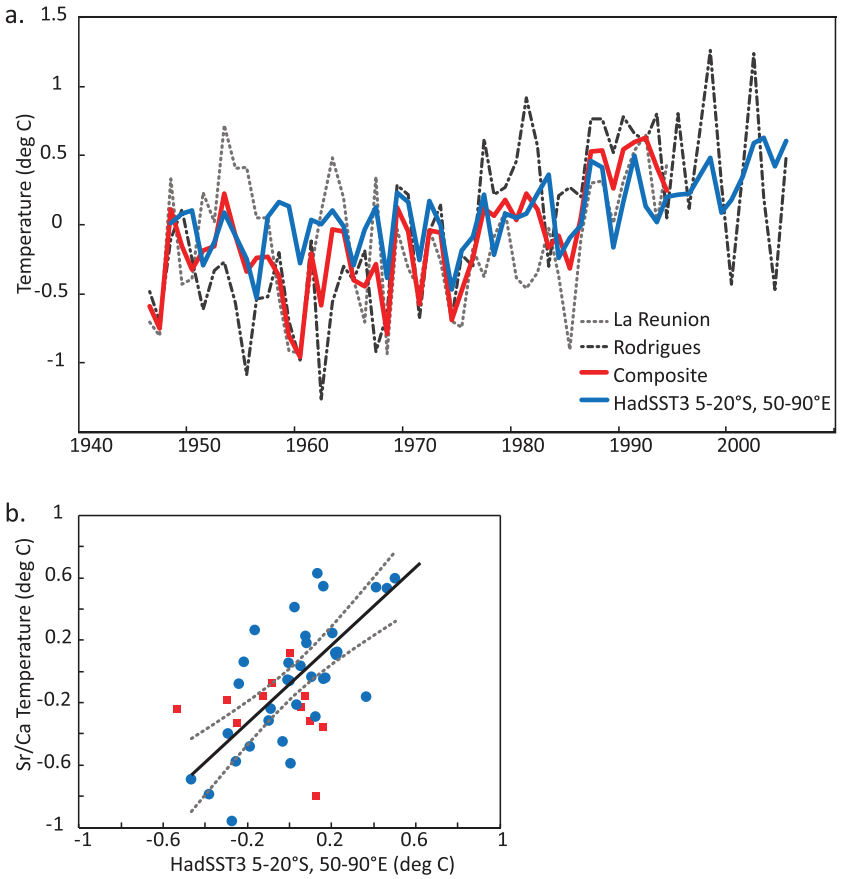

Figure 9. Composite coral Sr/Ca record from La Reunion and Rodrigues Island. (a) Annual mean Sr/Ca-temperature from Rodrigues (dash-dotted line) and La Reunion (dotted line) and composite Sr/Ca-temperatures compared with HadSST3 averaged over 50–90°E and 5–20°S. The Sr/Ca records have been centered by removing their mean and converted to temperature using −0.06 mmol/mol/1 °C. (b) OLS regression of annual mean composite Sr/Ca versus HadSST3 for 1948–1995 (red squares and blue circles, $r = 0.6$, $p < 0.1$, $N = 47$) and for 1960–1995 (blue circles, $r = 0.71$, $p < 0.01$, $N = 35$). See text for discussion.

relationship of −0.06 mmol/mol per 1 °C (Corrège, 2006). As an index of large-scale SST, HadSST3 data were averaged over the SW Indian Ocean basin (50–90°E, 5–20°S). HadSST3 was chosen because it is based on actual observations and corresponds well with twentieth century coral SST reconstructions from the tropical Indian Ocean, where more SST observations are available (Pfeiffer et al., 2017). Note that missing monthly mean SST data prevented the computation of annual average values prior to 1948.

Figure 9 compares the two single-core coral Sr/Ca-SST records and the composite reconstruction with HadSST3 for the SW Indian Ocean basin. Averaging the two single-core reconstructions improves the correlation with large scale SST ($r = 0.6$, $p < 0.01$ for 1948–1995 and $r = 0.71$, $p < 0.01$ for the better-observed and bias-free period from 1960 to 1995). The composite record also has a lower standard deviation (in °C units) than either of the two single records, and the slope of the composite coral SST-HadSST3 regression is not significantly different from one. These results support the use of coral Sr/Ca for large-scale temperature reconstructions. Averaging the cores appears to increase the large-scale climatic signal and reduces the noise. However, this approach does not provide any information on the source of the noise, that is, whether it derives from local climatic factors (in which case the Sr/Ca record would accurately portray reef-scale temperatures) or other nonclimatic artifacts such as vital effects (in which case coral Sr/Ca would deviate from reef-scale temperatures). Recent studies from the SW subtropical Indian Ocean suggest that coral Sr/Ca records from this region should be treated with some caution (Grove, Kasper, et al., 2013; Zinke et al., 2016). However, large-scale temperature reconstructions are possible if a careful validation of coral Sr/Ca reconstructions ensures their quality (e.g., DeLong et al., 2013; Zinke et al., 2016).

6. Summary and Conclusions

A paired coral $\delta^{18}O$ and Sr/Ca record has been developed from a La Reunion coral, covering the time period from 1913 to 1995. Monthly and annual mean coral Sr/Ca shows the expected temperature response. Annual mean coral Sr/Ca records year-to-year variations in SST and significantly correlates with historical SST data back to 1966, when the observational database is good. The validation of multidecadal variations in coral Sr/Ca is hampered by the sparse historical SST data in the SW Indian Ocean. The correlation between annual mean coral $\delta^{18}O$ and historical SST is zero, suggesting that the temperature contribution to coral $\delta^{18}O$ is small on time scales longer than the seasonal cycle. This confirms that coral $\delta^{18}O$ records primarily changes in $\delta^{18}O_{sw}$ and SSS.

Relative variations of $\delta^{18}O_{sw}$ are estimated from coral $\delta^{18}O$ by subtracting the temperature component inferred from coral Sr/Ca and from historical SSTs. In the midtwentieth century, $\delta^{18}O_{sw}$ shows a significant freshening with a magnitude of ~0.17–0.19‰. This translates into a freshening of ~0.7 psu. However, the timing of this shift differs depending on the temperature component subtracted from measured coral $\delta^{18}O$, from 1946 (historical SST data) to the late 1950s (coral Sr/Ca temperature), that is, by more than 10 years. The timing is important to understand its underlying causes. A freshening in 1946 may be driven by the PDO, which may influence the SEC via the ITF. A freshening in the late 1950s, as indicated by coral Sr/Ca, would suggest that other processes, possibly internal to the southern Indian Ocean basin, also play a role. For example, changes in the southern Indian Ocean wind field may modulate the position of the southern margin of the SEC. Further replication studies of paired coral $\delta^{18}O$ and Sr/Ca records are needed to address this issue.

A composite coral Sr/Ca record calculated from the La Reunion and Rodrigues Sr/Ca records correlates with large-scale SST in the SW tropical Indian Ocean. This suggests that it is possible to estimate large-scale SSTs in this region from carefully validated Sr/Ca records.

Acknowledgments
We thank the members of the TESTREEF program for assisting with drilling the Reunion coral core. Karin Kießling helped with Sr/Ca analysis. This study was funded by the DFG (PF 676/1-1 and PF 676 2-1). The coral Sr/Ca and $\delta^{18}O$ data generated in this study are available in the supporting information Data Set S1 and are archived at the NOAA NCDC World Data Center for Paleoclimatology (https://www.ncdc.noaa.gov/paleo-search/study/28130). Other data sets are sourced from the knmi climate explorer (https://climexp.knmi.nl).

References

Abram, N. J., Gagan, M. K., Cole, J. E., Hantoro, W. S., & Mudelsee, M. (2008). Recent intensification of tropical climate variability in the Indian Ocean. *Nature Geoscience*, *1*, 849–853.

Bingham, F. M., Foltz, G. R., & McPhaden, M. J. (2012). Characteristics of the seasonal cycle of surface layer salinity in the global ocean. *Ocean Science*, *8*(5), 915–929.

Cahyarini, S. Y., Pfeiffer, M., Nurhati, I. S., Aldrian, E., Dullo, W.-C., & Hetzinger, S. (2014). SST and salinity variations at the Indonesian throughflow exit passage over the 20th century via paired Timor coral $\delta^{18}O$ and Sr/Ca. *Journal of Geophysical Research: Oceans*, *119*, 4593–4604. https://doi.org/10.1002/2013JC009594

Cahyarini, S. Y., Pfeiffer, M., Timm, O., Dullo, W. C., & Schönberg, D. G. (2008). Reconstructing seawater $\delta^{18}O$ from paired coral $\delta^{18}O$ and Sr/Ca ratios: Methods, error analysis and problems, with examples from Tahiti (French Polynesia) and Timor (Indonesia). *Geochimica et Cosmochimica Acta*, *72*(12), 2841–2853. https://doi.org/10.1016/j.gca.2008.04.005

Charles, C. D., Hunter, D. E., & Fairbanks, R. G. (1997). Interaction between the ENSO and the Asian monsoon in a coral record of tropical climate. *Science*, *277*, 925–928.

Corrège, T. (2006). Sea surface temperature and salinity reconstruction from coral geochemical tracers. *Palaeogeography, Palaeoclimatology, Palaeoecology*, *232*(2), 408–428.

de Villiers, S., Greaves, M., & Elderfield, H. (2002). An intensity ratio calibration method for the accurate determination of Mg/Ca and Sr/Ca of marine carbonates by ICP-AES. *Geochemistry, Geophysics, Geosystems*, *3*(1), 1001. https://doi.org/10.1029/2001GC000169

DeLong, K. L., Quinn, T. M., Taylor, F. W., Shen, C.-C., & Lin, K. (2013). Improving coral-based paleoclimate reconstructions by replicating 350 years of coral Sr/Ca variations. *Palaeogeography, Palaeoclimatology, Palaeoecology*, *373*, 6–24.

Felis, T., Ionita, M., Rimbu, N., Lohmann, G., & Kölling, M. (2018). Mild and arid climate in the eastern Sahara-Arabian Desert during the late Little Ice Age. *Geophysical Research Letters*, *45*, 7112–7119. https://doi.org/10.1029/2018GL078617

Good, S. A., Martin, M. J., & Rayner, N. A. (2013). EN4: Quality controlled ocean temperature and salinity profiles and monthly objective analyses with uncertainty estimates. *Journal of Geophysical Research: Oceans*, *118*, 6704–6716. https://doi.org/10.1002/2013JC009067

Grove, C. A., Kasper, S., Zinke, J., Pfeiffer, M., Garbe-Schönberg, D., & Brummer, G.-J. A. (2013). Confounding effects of coral growth and high SST variability on skeletal Sr/Ca: Implications for coral paleothermometry. *Geochemistry, Geophysics, Geosystems*, *14*, 1277–1293. https://doi.org/10.1002/ggge.20095

Grove, C. A., Zinke, J., Peeters, F., Parl, W., Scheufen, T., Kapser, S., et al. (2013). Madagascar corals reveal a multidecadal signature of rainfall and river runoff since 1708. *Climate of the Past*, *9*, 641–656. https://doi.org/10.5194/cp-9-641-2013

Hammer, Ø., Harper, D. A. T., & Ryan, P. D. (2001). Past: Paleontological statistics software package for education and data analysis. *Palaeontologia Electronica*, *4*(1), 9.

Han, W., & McCreary, J. P. (2001). Modeling salinity distributions in the Indian Ocean. *Journal of Geophysical Research*, *106*(C1), 859–877.

Han, W., Vialard, J., McPhaden, M. J., Lee, T., Masumoto, V., Feng, M., & DeRuijter, W. P. M. (2014). Indian Ocean decadal variability. *Bulletin of the American Meteorological Society*, *95*(11), 1679–1703. https://doi.org/10.1175/BAMS-D-13-00028.1

Hendy, E. J., Gagan, M. K., Lough, J. M., McCulloch, M., & de Menocal, P. B. (2007). Impact of skeletal dissolution and secondary aragonite on trace element and isotopic climate proxies in Porites corals. *Paleoceanography*, *22*, PA4101. https://doi.org/10.1029/2007PA001462

Hennekam, R., Zinke, J., van Sebille, E., ten Have, M., Brummer, G.-J. A., & Reichart, G.-J. (2018). Cocos (Keeling) corals reveal 200 years of multidecadal modulation of southeast Indian Ocean hydrology by Indonesian throughflow. *Paleoceanography and Paleoclimatology*, *33*, 48–60. https://doi.org/10.1002/2017PA003181

Huang, B., Thorne, P. W., Banzon, V. F., Boyer, T., Chepurin, G., Lawrimore, J. H., et al. (2017). Extended Reconstructed Sea Surface Temperature version 5 (ERSSTv5), Upgrades, validations, and intercomparisons. *Journal of Climate*, *30*(20), 8179–8205. https://doi.org/10.1175/JCLI-D-16-0836.1

Juillet-Leclerc, A., & Schmidt, G. (2001). A calibration of the oxygen isotope paleothermometer of coral aragonite from *Porites*. *Geophysical Research Letters*, *28*(21), 4135–4138.

Kennedy, J. J., Rayner, N. A., Smith, R. O., Saunby, M., & Parker, D. E. (2011a). Reassessing biases and other uncertainties in sea-surface temperature observations since 1850, part 1: Measurement and sampling errors. *Journal of Geophysical Research*, *116*, D14103. https://doi.org/10.1029/2010JD015218

Kennedy, J. J., Rayner, N. A., Smith, R. O., Saunby, M. D., & Parker, E. (2011b). Reassessing biases and other uncertainties in sea-surface temperature observations since 1850, part 2: Biases and homogenization. *Journal of Geophysical Research*, *116*, D14104. https://doi.org/10.1029/2010JD015220

Kuhnert, H., Kuhlmann, H., Mohtadi, M., Meggers, H., Baumann, K.-H., & Pätzold, J. (2014). Holocene tropical western Indian Ocean sea surface temperatures in covariation with climatic changes in the Indonesian region. *Paleoceanography*, *29*, 423–437. https://doi.org/10.1002/2013PA002555

Melnichenko, O., Hacker, P., Maximenko, N., Lagerloef, G., & Potemra, J. (2014). Spatial optimal interpolation of Aquarius sea surface salinity: Algorithms and implementation in the North Atlantic. *Jtech*, *31*, 1583–1600. https://doi.org/10.1175/JTECH-D-13-00241.1

Melnichenko, O., Hacker, P., Maximenko, N., Lagerloef, G., & Potemra, J. (2015). Optimum interpolation analysis of Aquarius sea surface salinity. *Journal of Geophysical Research: Oceans*, *121*, 602–616. https://doi.org/10.1002/2015JC011343

Nidheesh, A. G., Lengaigne, M., Vialard, J., Unnikrishnan, A. S., & Dayan, H. (2013). Decadal and long-term sea level variability in the tropical Indo-Pacific Ocean. *Climate Dynamics*, *41*, 381–402. https://doi.org/10.1007/s00382-012-1463-4

Nurhati, I. S., Cobb, K. M., & Di Lorenzo, E. (2011). Decadal-scale SST and salinity variations in the central tropical pacific: Signatures of natural and anthropogenic climate change. *Journal of Climate*, *24*, 3294–3308. https://doi.org/10.1175/2011JCLI3852.1

Nyadjro, E. S., & Subrahmanyam, B. (2016). Spatial and temporal variability of central Indian Ocean salinity fronts observed by SMOS. *Remote Sensing of Environment*, *180*, 146–153. https://doi.org/10.1016/j.rse.2016.02.049

Pfeiffer, M., Dullo, W.-C., Zinke, J., & Garbe-Schönberg, D. (2009). Three monthly coral Sr/Ca records from the Chagos Archipelago covering the period of 1950–1995 A.D.: Reproducibility and implications for quantitative reconstructions of sea surface temperature variations. *International Journal of Earth Sciences*, *98*, 53–66. https://doi.org/10.1007/s00531-008-0326-z

Pfeiffer, M., Timm, O., Dullo, W. C., & Podlech, S. (2004). Oceanic forcing of interannual and multidecadal climate variability in the southwestern Indian Ocean: Evidence from a 160 year coral isotopic record (La Réunion, 55°E, 21°S). *Paleoceanography*, *19*, PA4006. https://doi.org/10.1029/2003PA000964

Pfeiffer, M., Zinke, J., Dullo, W.-C., Timm, O., Cahyarini, S. Y., Latif, M., & Weber, M. E. (2017). Indian Ocean corals reveal crucial role of World War II bias for twentieth century warming estimates. *Scientific Reports*, *7*, 14434. https://doi.org/10.1038/s41598-017-14352-6

Rayner, N. A., Parker, D. E., Horton, E. B., Folland, C. K., Alexander, L. V., Rowell, D. P., et al. (2003). Global analyses of sea surface temperature, sea ice, and night marine air temperature since the late nineteenth century. *Journal of Geophysical Research*, *108*(D14), 4407. https://doi.org/10.1029/2002JD002670

Reynolds, R. W., Rayner, N. A., Smith, T. M., Stokes, D. C., & Wang, W. (2002). An improved in situ and satellite SST analysis for climate. *Journal of Climate*, *15*, 1609–1625.

Roxy, M., Ritika, K., Terray, P., & Masson, S. (2014). The curious case of Indian Ocean warming. *Journal of Climate*, *27*(22), 8501–8509. https://doi.org/10.1175/JCLI-D-14-00471.1

Sayani, H., Cobb, K. M., DeLong, K., Hitt, N. T., & Druffel, E. R. M. (2019). Intercolony δ18O and Sr/Ca variability among Porites spp. corals at Palmyra Atoll: Towards more robust coral-based estimates of climate. *Geochemistry, Geophysics, Geosystems*. https://doi.org/10.1029/2019GC008420

Sayani, H. R., Cobb, K. M., Cohen, A. L., Elliott, W. C., Nurhati, I. S., Dunbar, R. B., et al. (2011). Effects of diagenesis on paleoclimate reconstructions from modern and young fossil corals. *Geochimica et Cosmochimica Acta*, *75*, 6361–6373. https://doi.org/10.1016/J.Gca.2011.08.026

Schmidt, G. A. (1998). Oxygen-18 variations in a global ocean model. *Geophysical Research Letters*, *25*(8), 1201–1204.

Schott, F. A., Xie, S.-P., & McCreary, J. P. Jr. (2009). Indian Ocean circulation and climate variability. *Reviews of Geophysics*, *47*, RG1002. https://doi.org/10.1029/2007RG000245

Schrag, D. P. (1999). Rapid analysis of high-precision Sr/Ca ratios in corals and other marine carbonates. *Paleoceanography*, *14*(2), 97–102.

Smodej, J., Reuning, L., Wollenberg, U., Zinke, J., Pfeiffer, M., & Kukla, P. A. (2015). Two-dimensional X-ray diffraction as a tool for the rapid, nondestructive detection of low calcite quantities in aragonitic corals. *Geochemistry Geophysics Geosystems*, *16*, 3778–3788. https://doi.org/10.1002/2015GC006009

Sprintall, J., Wijffels, S. E., Molcard, R., & Jaya, I. (2009). Direct estimates of the Indonesian Throughflow entering the Indian Ocean: 2004–2006. *Journal of Geophysical Research*, *114*, C07001. https://doi.org/10.1029/2008JC005257

Srivastava, R., Ramesh, R., Prakash, S., Anilkumar, N., & Sudhakar, M. (2007). Oxygen isotope and salinity variations in the Indian sector of the Southern Ocean. *Geophysical Research Letters*, *34*, L24603. https://doi.org/10.1029/2007GL031790

Thompson, D. W. J., Kennedy, J. J., Wallace, J. M., & Jones, P. D. (2008). A large discontinuity in the mid-twentieth century in observed global-mean surface temperature. *Nature*, *453*, 646–649. https://doi.org/10.1038/nature06982

Tierney, J. E., Abram, N. J., Anchukaitis, K. J., Evans, M. N., Giry, C., Kilbourne, K. H., et al. (2015). Tropical sea surface temperatures for the past four centuries reconstructed from coral archives. *Paleoceanography*, *30*, 226–252. https://doi.org/10.1002/2014PA002717

van Oldenborgh, G. J., & Burgers, G. (2005). Searching for decadal variations in ENSO precipitation teleconnections. *Geophysical Research Letters*, *32*, L15701. https://doi.org/10.1029/2005GL023110

Wainwright, L., Meyers, G., Wijffels, S., & Pigot, L. (2008). Change in the Indonesian throughflow with the climatic shift of 1976/77. *Geophysical Research Letters*, *35*, L03604. https://doi.org/10.1029/2007GL031911

Watanabe, T. K., Watanabe, T., Yamazaki, A., Pfeifer, M., & Claereboudt, M. R. (2019). Oman coral $\delta^{18}O$ seawater record suggests that Western Indian Ocean upwelling uncouples from the Indian Ocean Dipole during the global-warming hiatus. *Scientific Reports*, *9*, 1887. https://doi.org/10.1038/s41598-018-38429-y

Watanabe, T. K., Watanabe, T., Yamazaki, A., Pfeiffer, M., Garbe-Schönberg, D., & Claereboudt, M. R. (2017). Past summer upwelling events in the Gulf of Oman derived from a coral geochemical record. *Scientific Reports*, *7*, 4568. https://doi.org/10.1038/s41598-017-04865-5

Werdell, P. J., Franz, B. A., Bailey, S. W., Feldman, G. C., Boss, E., Brando, V. E., et al. (2013). Generalized ocean color inversion model for retrieving marine inherent optical properties. *Applied Optics*, *52*(10), 2019–2037. https://doi.org/10.1364/AO.52.002019

Woodruff, S. D., Worley, S. J., Lubker, S. J., Ji, Z., Eric Freeman, J., Berry, D. I., et al. (2011). ICOADS Release 2.5: Extensions and enhancements to the surface marine meteorological archive. *International Journal of Climatology*, *31*(7), 951–967. https://doi.org/10.1002/joc.2103

Zhang, Z., Falter, J., Lowe, R., Ivey, G., & McCulloch, M. (2013). Atmospheric forcing intensifies the effects of regional ocean warming on reef-scale temperature anomalies during a coral bleaching event. *Journal of Geophysical Research: Oceans*, *118*, 4600–4616. https://doi.org/10.1002/jgrc.203382013

Zhuang, W., Feng, M., Du, Y., Schiller, A., & Wang, D. (2013). Low-frequency sea level variability in the southern Indian Ocean and its impacts on the oceanic meridional transports. *Journal of Geophysical Research: Oceans*, *118*, 1302–1315. https://doi.org/10.1002/jgrc.20129

Zinke, J., Pfeiffer, M., Timm, O., Dullo, W.-C., Kroon, D., & Thomassin, B. (2008). Mayotte coral reveals hydrological changes in the western Indian Ocean between 1881 and 1994. *Geophysical Research Letters*, *35*, L23707. https://doi.org/10.1029/2008GL035634

Zinke, J., Reuning, L., Pfeiffer, M., Wassenburg, J. A., Hardman, E., Jhangeer-Khan, R., et al. (2016). A sea surface temperature reconstruction for the southern Indian Ocean trade wind belt from corals in Rodrigues Island (19°S, 63°E). *Biogeosciences*, *13*(20), 5827–5847. https://doi.org/10.5194/bg-13-5827-2016